

# Nonlinearity of vacuum Reggeons and exclusive diffractive production of vector mesons at HERA

*A.A. Godizov\**, *V.A. Petrov†*

*Institute for High Energy Physics, 142281 Protvino, Russia*

## Abstract

The processes of exclusive photo- and electroproduction of vector mesons  $\rho^0(770)$ ,  $\phi(1020)$  and  $J/\psi(3096)$  at collision energies  $30 \text{ GeV} < W < 300 \text{ GeV}$  and transferred momenta squared  $0 < -t < 2 \text{ GeV}^2$  are considered in the framework of a phenomenological Regge-eikonal scheme with nonlinear Regge trajectories in which their QCD asymptotic behavior is taken into account explicitly. By comparison of available experimental data from ZEUS and H1 Collaborations with the model predictions it is demonstrated that corresponding angular distributions and integrated cross sections in the above-mentioned kinematical range can be quantitatively described with use of two  $C$ -even vacuum Regge trajectories. These are the “soft” Pomeron dominating the high-energy reactions without a hard scale and the “hard” Pomeron giving an essential contribution to photo- and electroproduction of heavy vector mesons and deeply virtual electroproduction of light vector mesons.

## Introduction

The aim of this paper is to demonstrate that reactions of exclusive vector meson photo- and electroproduction can be described in the framework of a Regge-eikonal scheme (the general Regge-eikonal approach was developed in [1]) similar to that as for high-energy nucleon-nucleon scattering. One of the distinctive features of the proposed model is the use of nonlinear parametrizations for Regge trajectories in the diffraction region in which their QCD asymptotic behavior is taken into account explicitly. In essence, the behavior of Regge trajectories at large transferred momenta is a fact of fundamental importance: QCD does not permit linear trajectories. Hence, there emerges the problem of compatibility of nonlinearity of Regge trajectories following from QCD with available set of experimental data. The scheme proposed in [2] and

---

\*godizov@sirius.ihep.su

†Vladimir.Petrov@ihep.ru

applied in this paper partially solves this problem since in the framework of our approach phenomenological Regge trajectories in the diffraction region satisfy the QCD asymptotic relations explicitly.

The detailed discussion of the fundamental properties of Regge trajectories (such as their essential nonlinearity in the Euclidean domain) can be found in [2]. Here we limit ourselves by substantiating several useful relations.

Our viewpoint (by no means very original) is based on the conviction that QCD is the fundamental theory of strong interaction. So, in the limit of large negative values of the argument (equivalent to short distances) the exchange by any Reggeon must turn into exchange by some colour-singlet parton combination and the asymptotic behavior of Regge poles corresponding to exchanges by definite parton combinations can be determined. For example, if some Reggeon corresponds to exchange by the quark-antiquark pair ( $f_2$  Reggeon, etc.) in the range of the perturbative QCD validity we come to [3]

$$\alpha_{\bar{q}q}(t) = \sqrt{\frac{8}{3\pi}\alpha_s(\sqrt{-t})} + o(\alpha_s^{1/2}(\sqrt{-t})) \quad (1)$$

In the case of multigluon exchange one obtains [4]

$$\lim_{t \rightarrow -\infty} \alpha_{gg\dots g}(t) = 1 \quad (2)$$

and, in particular, for two-gluon exchange [5]

$$\alpha_{gg}(t) = 1 + \frac{12 \ln 2}{\pi} \alpha_s(\sqrt{-t}) + o(\alpha_s(\sqrt{-t})) \quad (3)$$

where  $\alpha_s(\mu) \equiv g_s^2(\mu)/4\pi$  is the QCD running coupling.

Besides, if we assume that  $\text{Im} \alpha(t + i0)$  increases slowly enough at  $t \rightarrow +\infty$  (for example, not faster than  $Ct \ln^{-1-\epsilon} t$ ,  $\epsilon > 0$ ) so that the dispersion relations with not more than one subtraction take place, i.e.

$$\alpha(t) = \alpha_0 + \frac{t}{\pi} \int_{t_T}^{+\infty} \frac{\text{Im} \alpha(t' + i0)}{t'(t' - t)} dt',$$

and  $\text{Im} \alpha(t + i0) \geq 0$  at  $t \geq t_T > 0$  we obtain

$$\frac{d^n \alpha(t)}{dt^n} > 0 \quad (t < t_T, n = 1, 2, 3, \dots). \quad (4)$$

It is usually assumed that for the true Regge trajectories relations (4) are fulfilled [6].<sup>1</sup>

In [2], it was demonstrated that taking into account physical restrictions (1), (2), (4) allows us to describe the diffractive pattern of high-energy nucleon-nucleon scattering in the framework of the minimal phenomenological Regge-eikonal model with only three (nonlinear) Regge trajectories (soft Pomeron and two secondary Reggeons).<sup>2</sup>

<sup>1</sup>Note that the amplitude depends explicitly on the functional form of the Regge trajectories only (not on their derivatives). So, for the phenomenological approximation it is sufficient to use some functions monotonous with one or several first derivatives.

<sup>2</sup>One could wonder if the nonlinearity of Regge trajectories related to high- $t$  behavior is so much important for diffractive scattering which occurs mainly at quite small transferred momenta. Isn't it more economical to deal with much more simple and convenient in many respects linear approximation  $\alpha(t) \approx \alpha(0) + \alpha'(0)t$ ? In Ref. [2], we demonstrated that such an approximation is valid only in quite a narrow interval of  $t$  (e.g.  $|t| < 0.3 \text{ GeV}^2$  for high-energy  $pp$  scattering).

Below we will show that such an approach also allows us to describe available data on high-energy ( $W > 30 \text{ GeV}$ ) exclusive vector meson photo- and electroproduction in the framework of the similar model, using only two  $C$ -even vacuum Regge trajectories, namely, soft and hard Pomerons (here we follow the pattern of Donnachie and Landshoff [7]). The soft Pomeron trajectory is the same as for the diffractive nucleon-nucleon scattering (in accordance with the requirement of universality of Regge trajectories) and the hard Pomeron trajectory, lying much higher than the soft one in the Euclidean domain (see Fig. 1), has the asymptotic behaviour (3) (in accordance with the fact that at high transfers the high-energy scattering amplitude is dominated by two-gluon exchange). The “invisibility” of the hard Pomeron in the elastic diffraction may be explained by the fact that at available energies its contribution to the on shell eikonal is suppressed by the soft Pomeron due to the disparity in on shell residues  $\beta_H(t) \ll \beta_P(t)$  (subscripts “ $H$ ” and “ $P$ ” correspond to hard and soft) in the nonperturbative regime.

## The model

We will treat the processes of exclusive vector meson production from the standpoint of the vector-dominance model (VDM) [8] in which the incoming photon fluctuates into a virtual vector meson which, in turn, scatters from the target proton. According to the so-called hypothesis of  $s$ -channel helicity conservation (the adequacy of this approximation is confirmed by numerous experimental data on helicity effects [9, 10, 11]) the cross section of reaction  $\gamma^* + p \rightarrow V + p$  is dominated by the nonflip helicity amplitude which can be represented in the form

$$T_{\gamma^*p \rightarrow Vp}^\lambda(W^2, t, Q^2) = \sum_{V'} C_{V'}^\lambda(Q^2) T_{V'^*p \rightarrow Vp}^\lambda(W^2, t, Q^2) \quad (5)$$

where the sum is taken over all neutral vector mesons.  $C_{V'}^\lambda(Q^2)$  is the coefficient of vector dominance dependent on the type of vector meson  $V'$ , helicity  $\lambda$  and virtuality  $Q^2$  of the incoming photon.  $T_{V'^*p \rightarrow Vp}^\lambda(W^2, t, Q^2)$  is the diffractive hadronic amplitude with Regge-eikonal structure (the applicability of the Regge-eikonal approach to the hadronic reactions with off shell particles is grounded in [12]).

It is known that for small enough values of  $t$  the diagonal coupling of vacuum Reggeons to hadrons is much stronger than the off diagonal coupling (for example, elastic proton-proton scattering has a considerably larger cross section than diffractive excitation of  $N(1470)$  in the proton-proton collisions). So, in the high-energy range ( $W > 30 \text{ GeV}$ ) where vacuum exchanges exceed the nonvacuum ones (the main indication of such an exceeding is the manifest growth of integrated cross sections with the collision energy increase) the so-called “diagonal approximation” of (5) may be used

$$T_{\gamma^*p \rightarrow Vp}^\lambda(W^2, t, Q^2) = C_V^\lambda(Q^2) T_{V^*p \rightarrow Vp}(W^2, t, Q^2) \quad (6)$$

(conversely, for a consistent description of the data at  $W < 30 \text{ GeV}$  the contribution from nonvacuum Reggeons must be taken into account and approximation (6) becomes invalid). Here we must note that recent measurements by ZEUS Collaboration [9, 10, 11] did not reveal patent dependence on  $t$  and  $W$  of the ratio of differential cross sections for the cases of longitudinally and transversely polarized incoming photon and this is the reason why we have omitted the superscript  $\lambda$  for  $T_{V^*p \rightarrow Vp}(W^2, t, Q^2)$  in (6). In other words, we presume that spin phenomena

related to the dependence of  $T_{V^*p \rightarrow Vp}(W^2, t, Q^2)$  on helicities of incoming and outgoing particles are much more fine effects than diffractive scattering itself and further deal only with quantities averaged over spin states.

According to (6) and Regge theory [6] the pole contribution of any  $C$ -even Reggeon  $R$  to the amplitude  $T_{\gamma^*p \rightarrow Vp}^\lambda(W^2, t, Q^2)$  has the form (the use of the designation  $\delta$  for the pole contribution is caused by the subsequent use of the Regge-eikonal scheme; see below)

$$C_V^\lambda(Q^2)\delta_R^{V^*}(W^2, t, Q^2) = C_V^\lambda(Q^2)\Gamma_R^{V^*V}(t, Q^2)\Gamma_R^{pp}(t) \left( i + \text{tg} \frac{\pi(\alpha_R(t) - 1)}{2} \right) \left( \frac{W^2}{W_0^2} \right)^{\alpha_R(t)}$$

where  $W_0 \equiv 1 \text{ GeV}$ ,  $\alpha_R(t)$  is the Reggeon trajectory, and  $\Gamma_R^{V^*V}(t, Q^2)$ ,  $\Gamma_R^{pp}(t)$  are the Reggeon form factors of participating particles.

The VDM in its simplest form gives [8]

$$C_V^{\pm 1}(Q^2) = \sqrt{\frac{3\Gamma_{V \rightarrow e^+e^-}}{\alpha_e M_V}} \frac{M_V^2}{M_V^2 + Q^2}, \quad \left( \frac{C_V^0(Q^2)}{C_V^{\pm 1}(Q^2)} \right)^2 = \frac{Q^2}{M_V^2}$$

where  $M_V$  is the vector meson mass,  $\alpha_e = \frac{1}{137}$  is the electromagnetic coupling, and  $\Gamma_{V \rightarrow e^+e^-}$  is the width of the vector meson decay to the electron-positron pair. However, these relations contradict both the experimental data on  $Q^2$  dependence of the ratio  $R(Q^2) = \frac{\sigma_{\gamma^*p \rightarrow Vp}^0}{\sigma_{\gamma^*p \rightarrow Vp}^{\pm 1}} \approx \left( \frac{C_V^0(Q^2)}{C_V^{\pm 1}(Q^2)} \right)^2$  [9, 10, 11] and the dimensional counting rules [13] according to which functions  $Q^2\Gamma_R^{V^*V}(t, Q^2)$ ,  $Q^2C_V^\lambda(Q^2)\Gamma_R^{V^*V}(t, Q^2)$ , and, hence,  $C_V^\lambda(Q^2)$  must exhibit moderate (nonpower-like)  $Q^2$  behavior.

To resolve this conflict we have to modify the VDM coefficients

$$C_V^\lambda(Q^2) = \sqrt{\frac{3\Gamma_{V \rightarrow e^+e^-}}{\alpha_e M_V}} \frac{M_V^2}{M_V^2 + Q^2} F_V^\lambda(Q^2) \quad (7)$$

and thus

$$C_V^\lambda(Q^2)\delta_R^{V^*}(W^2, t, Q^2) = \sqrt{\frac{3\Gamma_{V \rightarrow e^+e^-}}{\alpha_e M_V}} \frac{M_V^2}{M_V^2 + Q^2} \times \\ \times F_V^\lambda(Q^2)\Gamma_R^{V^*V}(t, Q^2)\Gamma_R^{pp}(t) \left( i + \text{tg} \frac{\pi(\alpha_R(t) - 1)}{2} \right) \left( \frac{W^2}{W_0^2} \right)^{\alpha_R(t)}$$

where, for any virtual photon spin state  $\lambda$ ,  $F_V^\lambda(-M_V^2) = 1$ , and function  $F_V^\lambda(Q^2)\Gamma_R^{V^*V}(t, Q^2)$  exhibits nonsteep  $Q^2$  behavior.

Further on, we will concentrate on the diffractive pattern ( $t$  dependence) of exclusive vector meson production and its evolution with collision energy ( $W$  dependence). Since the second factor in the right-hand side of (6) nearly does not depend on  $\lambda$  we may consider only cross sections averaged over helicities of external particles. The averaged pole contribution of a Reggeon  $R$  to the amplitude takes the form

$$\bar{C}_V(Q^2)\delta_R^{V^*}(W^2, t, Q^2) = \sqrt{\frac{3\Gamma_{V \rightarrow e^+e^-}}{\alpha_e M_V}} \frac{M_V^2}{M_V^2 + Q^2} \times \quad (8)$$

$$\times \bar{\Gamma}_R^{V^*V}(t, Q^2) \Gamma_R^{pp}(t) \left( i + \text{tg} \frac{\pi(\alpha_R(t) - 1)}{2} \right) \left( \frac{W^2}{W_0^2} \right)^{\alpha_R(t)}$$

where

$$\bar{C}_V(Q^2) \equiv \sqrt{\frac{3\Gamma_{V \rightarrow e^+e^-}}{\alpha_e M_V} \frac{M_V^2}{M_V^2 + Q^2}} \bar{F}_V(Q^2), \quad \bar{F}_V(Q^2) \equiv \sqrt{\frac{1}{3} \sum_{\lambda} (F_V^{\lambda}(Q^2))^2},$$

$$\bar{\Gamma}_R^{V^*V}(t, Q^2) \equiv \bar{F}_V(Q^2) \Gamma_R^{V^*V}(t, Q^2), \quad \bar{\Gamma}_R^{V^*V}(t, -M_V^2) \equiv \Gamma_R^{VV}(t).$$

In a well-known paper [14], it was argued that  $\bar{F}_V(Q^2) = 1 + \frac{Q^2}{m_{V0}^2}$  where  $m_{V0}$  is the vector meson “bare” mass. At infinite values of  $m_{V0}$  the usual form of the current-field relation takes place. An interesting feature of this variant is a possibility to extend the VDM applicability for arbitrarily high  $Q^2$ . We do not fix the concrete functional form of  $\bar{F}_V(Q^2)$  (it does not help to determine  $Q^2$  behavior of  $\bar{\Gamma}_R^{V^*V}(t, Q^2)$  because of the absence of detailed information on  $Q^2$  dependence of  $\Gamma_R^{V^*V}(t, Q^2)$ ). According to the dimensional counting rules [13]  $\Gamma_R^{V^*V}(t, Q^2) \sim Q^{-2}$  at high  $Q^2$  (we point out that such a behavior implies the violation of Bjorken scaling [15]), so  $\bar{\Gamma}_R^{V^*V}(t, Q^2)$  must exhibit slow evolution with  $Q^2$ .

After these general remarks we can proceed to construct the scattering amplitude. It is well known that for soft reactions such as elastic nucleon-nucleon scattering or light vector meson photoproduction the introduction of only one trajectory with intercept higher than unity is necessary (the soft Pomeron). But in the processes with a hard scale (for example, photon virtuality or/and heavy vector meson mass) the rise of the cross sections with the collision energy becomes noticeably faster than in the soft ones and so there emerges the question if there exists one or several extra Reggeons lying higher than the soft Pomeron but with entirely suppressed residue(s) in the nonperturbative regime [16].<sup>3</sup>

Below we will use the minimal phenomenological scheme based on the idea of Donnachie and Landshoff [7, 17] that only one extra Reggeon with the intercept much higher than the soft Pomeron’s one is needed. The difference between our realization of this idea and the Donnachie-Landshoff model lies in a choice of the functional form of Regge trajectories since the authors [7, 17] insist on the strict linearity of the trajectories while we use essentially nonlinear parametrizations with asymptotic behavior following from QCD (cf. the footnote 2).

We assume that at collision energies  $W > 30 \text{ GeV}$  we may neglect contributions from secondary Reggeons. In this case the minimal vacuum exchange off shell eikonal (the sum of one-Reggeon-exchange amplitudes [1]) takes the form

$$\begin{aligned} \bar{C}_V(Q^2) \delta^{V^*}(W^2, t, Q^2) &\equiv \delta^*(W^2, t, Q^2) = \delta_P^*(W^2, t, Q^2) + \delta_H^*(W^2, t, Q^2) = \\ &= \sqrt{\frac{3\Gamma_{V \rightarrow e^+e^-}}{\alpha_e M_V} \frac{M_V^2}{M_V^2 + Q^2}} \left[ \left( i + \text{tg} \frac{\pi(\alpha_P(t) - 1)}{2} \right) \bar{\Gamma}_P^{V^*V}(t, Q^2) \Gamma_P^{pp}(t) \left( \frac{W^2}{W_0^2} \right)^{\alpha_P(t)} + \right. \\ &\quad \left. + \left( i + \text{tg} \frac{\pi(\alpha_H(t) - 1)}{2} \right) \bar{\beta}_H^{V^*}(t, Q^2) \left( \frac{W^2}{W_0^2} \right)^{\alpha_H(t)} \right], \end{aligned} \quad (9)$$

---

<sup>3</sup>Introducing extra trajectories may seem a violation of the Occam razor principle. Actually, we did try a version with a single Pomeron but in this case one needs negative and growing with  $Q^2$  residues for secondary trajectories ( $f_2$  Reggeon etc.). The last circumstance looks too counter-intuitive and a hard Pomeron seems inevitable.

where  $\alpha_P(t)$ ,  $\alpha_H(t)$  are Regge trajectories of the soft and hard Pomerons,  $\bar{\Gamma}_P^{V^*V}(t, Q^2)$  and  $\Gamma_P^{pp}(t)$  are the soft Pomeron form factors of outgoing vector meson and proton, and  $\bar{\beta}_H^{V^*}(t, Q^2) \equiv \bar{\Gamma}_H^{V^*V}(t, Q^2)\Gamma_H^{pp}(t)$  is the Regge residue of the hard Pomeron. Factors  $\bar{\Gamma}_H^{V^*V}(t, Q^2)$  and  $\Gamma_H^{pp}(t)$  are absorbed into an overall hard residue  $\bar{\beta}_H^{V^*}(t, Q^2)$  since the hard Pomeron gives no noticeable contribution to the eikonal of nucleon-nucleon scattering at accessible energies and so we can not separately fix the form factor  $\Gamma_H^{pp}(t)$  from the data on high-energy proton-(anti)proton diffraction.

The corresponding on-shell eikonal of elastic  $Vp$  scattering is of the form:

$$\delta^V(W^2, t) = \left( i + \text{tg} \frac{\pi(\alpha_P(t) - 1)}{2} \right) \Gamma_P^{VV}(t) \Gamma_P^{pp}(t) \left( \frac{W^2}{W_0^2} \right)^{\alpha_P(t)} + \quad (10)$$

$$+ \left( i + \text{tg} \frac{\pi(\alpha_H(t) - 1)}{2} \right) \beta_H^V(t) \left( \frac{W^2}{W_0^2} \right)^{\alpha_H(t)}.$$

Since Regge trajectories are universal functions of one argument, i.e. depend neither on the type of the process in which the corresponding Reggeons contribute nor on the virtualities of the incoming particles, we will use, for the description of exclusive diffractive production of vector mesons, the same phenomenological expressions for the soft Pomeron trajectory and the corresponding form factor of the proton as we did for high-energy nucleon-nucleon scattering [2]:

$$\alpha_P(t) = 1 + p_1 \left[ 1 - p_2 t \left( \text{arctg}(p_3 - p_2 t) - \frac{\pi}{2} \right) \right], \quad (11)$$

$$\beta_P^{pp}(t) = (\Gamma_P^{pp}(t))^2 = B_P e^{b_P t} (1 + d_1 t + d_2 t^2 + d_3 t^3 + d_4 t^4)$$

(the values of free parameters obtained by fitting the data on proton-(anti)proton angular distributions are represented in Table 1).

$p_1$	0.123	$d_1$	$0.43 \text{ GeV}^{-2}$
$p_2$	$1.58 \text{ GeV}^{-2}$	$d_2$	$0.39 \text{ GeV}^{-4}$
$p_3$	0.15	$d_3$	$0.051 \text{ GeV}^{-6}$
$B_P$	43.5	$d_4$	$0.035 \text{ GeV}^{-8}$
$b_P$	$2.4 \text{ GeV}^{-2}$		

Table 1: Parameters for  $\alpha_P(t)$  and  $\Gamma_P^{pp}(t)$  obtained by fitting the data on proton-(anti)proton angular distributions.

The hard Pomeron trajectory is chosen in the form similar to the one used in [18] for the  $\rho$  Reggeon

$$\alpha_H(t) = 1 + \frac{1}{A_H + \left[ \frac{12 \ln 2}{\pi} \alpha_s(\sqrt{-t + c_H}) \right]^{-1}} \quad (12)$$

where

$$\alpha_s(\mu) \equiv \frac{4\pi}{11 - \frac{2}{3}n_f} \left( \frac{1}{\ln \frac{\mu^2}{\Lambda^2}} + \frac{1}{1 - \frac{\mu^2}{\Lambda^2}} \right)$$

is the so-called (one-loop) analytical QCD effective coupling constant [19],  $n_f = 3$  is the number of quark flavors taken into account,  $\Lambda = \Lambda^{(3)} = 0.346 \text{ GeV}$  is the QCD dimensional parameter (the value was taken from [20]) and  $A_H$  and  $c_H$  are free parameters. Note that our approximations to the soft and hard Pomerons satisfy asymptotic relations (2) and (3) thus corresponding to multi- and two-gluon exchanges at high transferred momenta.

Form-factor  $\bar{\Gamma}_P^{V^*V}(t, Q^2)$  and residue  $\bar{\beta}_H^{V^*}(t, Q^2)$  are assumed to have approximately an exponential form for any value of  $Q^2$  and small enough values of  $t$

$$\bar{\Gamma}_P^{V^*V}(t, Q^2) = B_P^V(Q^2)e^{b_P^V(Q^2)t}, \quad \bar{\beta}_H^{V^*}(t, Q^2) = B_H^V(Q^2)e^{b_H^V(Q^2)t} \quad (V = \rho, \phi, J/\psi). \quad (13)$$

Here  $B_P^V(Q^2)$  characterizes the effective intensity of the interaction between vector meson  $V$  and soft Pomeron and  $b_P^V(Q^2)$  is associated with the corresponding effective radius of interaction.

To obtain angular distributions we substitute (11), (12), (13) into (9), (10) and proceed via Fourier-Bessel transformation

$$\delta^*(W^2, b, Q^2) = \frac{1}{16\pi W^2} \int_0^\infty d(-t) J_0(b\sqrt{-t}) \delta^*(W^2, t, Q^2), \quad (14)$$

$$\delta^V(W^2, b) = \frac{1}{16\pi W^2} \int_0^\infty d(-t) J_0(b\sqrt{-t}) \delta^V(W^2, t)$$

to the impact parameter representation.

For obtaining the full amplitude we take use of an extended (off shell) eikonal representation [12]

$$\begin{aligned} T_{\gamma^*p \rightarrow Vp}(W^2, b, Q^2) &= \frac{\delta^*(W^2, b, Q^2)}{\delta^V(W^2, b)} T_{Vp \rightarrow Vp}(W^2, b) = \\ &= \frac{\delta^*(W^2, b, Q^2)}{\delta^V(W^2, b)} \frac{e^{2i\delta^V(W^2, b)} - 1}{2i} = \delta^*(W^2, b, Q^2) + i\delta^*(W^2, b, Q^2)\delta^V(W^2, b) + \dots \end{aligned} \quad (15)$$

(here  $T_{Vp \rightarrow Vp}(W^2, b) = \frac{e^{2i\delta^V(W^2, b)} - 1}{2i}$  is the ‘‘eikonalized’’ (unitarized) amplitude of elastic  $Vp$ -scattering). The inverse Fourier-Bessel transformation

$$T_{\gamma^*p \rightarrow Vp}(W^2, t, Q^2) = 4\pi W^2 \int_0^\infty db^2 J_0(b\sqrt{-t}) T_{\gamma^*p \rightarrow Vp}(W^2, b, Q^2) \quad (16)$$

gives the full amplitude in the momentum representation (during numerical calculating integrals from (14), (16) we approximate upper limits of integration by  $8 \text{ GeV}^2$  and  $250 \text{ GeV}^{-2} \approx (3 \text{ fm})^2$  correspondingly) and then is used for the differential cross section

$$\frac{d\sigma_{\gamma^*p \rightarrow Vp}}{dt} = \frac{|T_{\gamma^*p \rightarrow Vp}(W^2, t, Q^2)|^2}{16\pi W^4}. \quad (17)$$

A different way of unitarizing off shell vector meson production amplitude was exploited in [21].

# The description of experimental data

Turn to the description of experimental data on exclusive diffractive production of vector mesons (the description of available angular distributions in the framework of another phenomenological approaches without “unitarization” can be found in [17, 22, 23, 24, 25]). At the very start we must note that because of the absence of high-energy data on elastic  $Vp$  scattering we have to make an assumption that  $\Gamma_P^{VV}(t) = \bar{\Gamma}_P^{V^*V}(t, -M_V^2) \approx \bar{\Gamma}_P^{V^*V}(t, 0)$  and  $\beta_H^V(t) = \bar{\beta}_H^{V^*}(t, -M_V^2) \approx \bar{\beta}_H^{V^*}(t, 0)$ . Below, it will be shown that corresponding quantities change very slowly with  $Q^2$  (in accordance with the dimensional counting rules [13]) and, so, such an approximation seems to be justified from the phenomenological point of view. In other words, for all reactions we will determine, at first, the on-shell eikonal  $\delta^V(W^2, t)$  from the data on photoproduction and then proceed to electroproduction of the considered vector meson. In accordance with experimental data the cross sections of exclusive production are obtained by integration over  $0 < -t < 0.6 \text{ GeV}^2$  for light mesons, over  $0 < -t < 1.25 \text{ GeV}^2$  for the photoproduction of  $J/\psi$ , and over  $0 < -t < 1.0 \text{ GeV}^2$  for the electroproduction of  $J/\psi$ .

We start from the consideration of exclusive production of  $\phi$  meson [26, 10]. Since the main set of corresponding data on angular distributions and integrated cross sections is concentrated in the region of not very high energies  $W < 140 \text{ GeV}$  and photon virtualities  $Q^2 < 14 \text{ GeV}^2$ , and experimental errors are rather large we can significantly simplify our phenomenological model by neglecting the contribution of the hard Pomeron (i.e. we put  $\bar{\beta}_H^{\phi^*}(t, Q^2) \approx 0$ ) not only at  $Q^2 \approx 0$  but also at all other values. Moreover, for  $Q^2 > 2 \text{ GeV}^2$  we will neglect the  $t$  dependence of  $\bar{\Gamma}_P^{\phi^*\phi}(t, Q^2)$  by putting  $b_P^\phi(Q^2) \approx 0$  (such an approximation implies that at  $Q^2 > 2 \text{ GeV}^2$  soft Pomeron interacts with pointlike objects inside  $\phi$  (in accord with the parton model) and  $t$  dependence of the corresponding Regge residue is entirely determined by the form factor  $\Gamma_P^{pp}(t)$ ). So for all nonzero values of  $Q^2$  we will have only one free parameter,  $B_P^\phi(Q^2)$ , since  $\alpha_P(t)$  and  $\Gamma_P^{pp}(t)$  are fixed from the data on nucleon-nucleon scattering.

The results of fitting the data are represented in Table 2 and Figs. 2–4. These figures show that our quite rough approximation provides the data description of a satisfactory quality especially for low values of  $Q^2$  (see Fig. 3), pointing to the fact that the soft Pomeron dominates even at nonzero photon virtualities and the contribution from the hard Pomeron lies within experimental errors. Figures 3, 4 also demonstrate that, in general, neglecting absorptive corrections (i.e. Regge cuts contribution) is inadmissible.

$Q^2, \text{ GeV}^2$	0.0	2.4	3.6	5.0	6.5	9.2	13.0	19.7
$B_P^\phi(Q^2)$	3.1	2.8	2.77	2.75	2.73	2.72	2.7	2.3
$b_P^\phi(Q^2), \text{ GeV}^{-2}$	0.6	0 (fixed)						
$\langle  t  \rangle_{W=75 \text{ GeV}}, \text{ GeV}^2$	0.13	0.20						

Table 2: Results of fitting the data on reaction  $\gamma^* + p \rightarrow \phi + p$ .

In accordance with remarks on the  $Q^2$ -dependence of  $\bar{\Gamma}_P^{V^*V}(t, Q^2)$  in the previous section,  $B_P^\phi(Q^2)$  changes rather slowly with  $Q^2$ . Also in Table 2 the average value of  $|t|$  at  $W = 75 \text{ GeV}$  is exhibited.

The amount and the quality of data on  $J/\psi$  electroproduction [27, 9] allow us to neglect neither the hard Pomeron’s contribution nor the  $t$  dependence of  $\bar{\Gamma}_P^{J/\psi^* J/\psi}(t, Q^2)$ . The results



of fitting are represented in Tab. 3 and Figs. 5—9. For the  $J/\psi$  photoproduction we obtain  $\chi^2 = 194$  over 114 experimental points. The evolution of  $\langle |t| \rangle$  (which is related to the transverse interaction radius,  $R^2 \sim \langle |t| \rangle^{-1}$ ) at fixed  $W$  ( $W = 90 \text{ GeV}$ ) is rather slow at all values of  $Q^2$  due to the fact that even at  $Q^2 \approx 0$  the perturbative regime takes place because of presence of the hard scale  $M_{J/\psi}$ .

$Q^2, \text{ GeV}^2$	0.0	3.2	7.0	16.0	22.4
$B_P^{J/\psi}(Q^2)$	0.25	0.23	0.21	0.19	0.18
$b_P^{J/\psi}(Q^2), \text{ GeV}^{-2}$	0.3	0.3	0.25	0.2	0.2
$B_H^{J/\psi}(Q^2)$	0.22	0.21	0.2	0.19	0.185
$b_H^{J/\psi}(Q^2), \text{ GeV}^{-2}$	1.3	1.3	1.25	1.2	1.2
$\langle  t  \rangle_{W=90 \text{ GeV}}, \text{ GeV}^2$	0.25	0.25	0.26	0.27	0.27
$A_H$	2.9				
$c_H, \text{ GeV}^2$	0.1				

Table 3: Results of fitting the data on reaction  $\gamma^* + p \rightarrow J/\psi + p$ .

The slow evolution of  $B_P^{J/\psi}(Q^2)$  and  $B_H^{J/\psi}(Q^2)$  and the decreasing of  $b_P^{J/\psi}(Q^2)$  and  $b_H^{J/\psi}(Q^2)$  with  $Q^2$  is also in full accordance with the aforesaid. The hard Pomeron trajectory is compared with the soft Pomeron one in Fig. 1. We point out that besides the fact that the phenomenological trajectory  $\alpha_H(t)$  has the Kirschner-Lipatov (two-gluon) asymptotics (3), its intercept  $\alpha_H(0) \approx 1.292$  almost coincides with a rough estimation of the lower bound for its value obtained in [28]. So, in the diffraction region the hard Pomeron contribution to the real part of the eikonal is comparable with its contribution to the imaginary part in accordance with more general theoretical predictions [29].

$Q^2, \text{ GeV}^2$	0.0	2.5	3.7	5.0	6.0	8.0	11.9	13.5	19.7	32.0	41.0
$B_P^{\rho^0}(Q^2)$	3.68	3.5	3.6	3.3	3.2	3.0	2.6	2.5	2.0	1.7	1.5
$b_P^{\rho^0}(Q^2), \text{ GeV}^{-2}$	0.8	0.3 (fixed)									
$B_H^{\rho^0}(Q^2)$	0 (fixed)	0.5	0.6	0.7	0.8	0.9	1.0	1.0	1.2	1.1	1.0
$b_H^{\rho^0}(Q^2), \text{ GeV}^{-2}$		1.3 (fixed)									

Table 4: Results of fitting the data on reaction  $\gamma^* + p \rightarrow \rho^0 + p$ .

At last, after determining the hard Pomeron trajectory we can describe the phenomenology of exclusive production of  $\rho^0$  [30, 11]. For the case of photoproduction,  $Q^2 \approx 0$ , we can neglect the contribution from the hard Pomeron. However, high quality of the data on integrated cross sections at nonzero  $Q^2$  does not allow us to do this for the deeply virtual electroproduction. Besides, determination of  $t$  slopes of  $\bar{\beta}_H^{\rho^0*}(t, Q^2)$  and  $\bar{\Gamma}_P^{\rho^0*}(t, Q^2)$  is quite a hard task because of little amount and rather poor-quality data on the electroproduction angular distributions. So, for an unambiguous description we put the values of these slopes at nonzero  $Q^2$  equal to those for  $J/\psi$ -photoproduction, i.e.  $b_P^{\rho^0}(Q^2) \approx b_P^{J/\psi}(0) = 0.3 \text{ GeV}^{-2}$  and  $b_H^{\rho^0}(Q^2) \approx b_H^{J/\psi}(0) = 1.3 \text{ GeV}^{-2}$ .

The results of the fitting data are represented in Table 4 and Figs. 10—12.

At the end of this section we would like to emphasize that the main success of the used model consists in a satisfactory description of electroproduction of  $\phi$  meson at  $Q^2 = 5 \text{ GeV}^2$  (Fig. 3: 1 free parameter versus 35 points) and photoproduction of  $J/\psi$  meson (Figs. 5, 6, 7: 6 free parameters versus 114 points). All other sets of data at fixed  $Q^2$  do not, in fact, allow unambiguous verification of validity of our Regge trajectories because of the insufficient amount of data on angular distributions (the data on electroproduction of  $\rho^0$  and  $J/\psi$  do not even allow us to fit parameters  $b_P^V(Q^2)$  and  $b_H^V(Q^2)$  unambiguously).

## Relation to other models

Two main features of our approach are the use of an eikonalized (unitarized) expression for the scattering amplitude and the exploitation of the essentially nonlinear parametrizations of Regge trajectories with explicit QCD asymptotic behavior.

Although there exists a whole sea of papers devoted to the description of  $W$  and  $Q^2$  evolution of integrated cross sections and structure functions, only few of them deal with diffractive pattern ( $t$  dependence) of the scattering amplitude. However, angular distributions contain very valuable information about the geometry of the interaction region and so they are more important quantities than integrated cross sections and structure functions. The papers which deal with this subject can be conventionally sorted into two groups.

The first group consists of the purely phenomenological works. In [22], the so-called ‘‘dipole Pomeron model’’ is used with the soft Pomeron as a double Regge pole with a square root threshold singularity. In [23], the model of dual amplitudes with Mandelstam analyticity (DAMA) with a square root leading singularity is used for the description of the  $J/\psi$  photoproduction. These two approaches, in fact, do not imply the concrete functional dependence of Regge trajectories (the authors of these papers use nonlinear parametrizations for Regge trajectories) and so are not in contradiction of principle with the requirement for Reggeons to have a QCD asymptotic behavior. In [17], the usual Born approximation for the scattering amplitude is used with postulated strictly linear Regge trajectories. We do not share this point of view since we consider the consistency with QCD (which implies nonlinearity) more important than quite an arbitrary hypothesis about strict linearity.

The second group consists of two papers [24, 25] exploiting the ‘‘colour dipole model’’ with a main hypothesis that if the incoming photon is of high virtuality or the outgoing vector meson is of high mass then the photon fluctuates into a quark-antiquark pair which scatters elastically off the proton and, at last, recombines into the vector meson. The main advantage of this approach is that it allows us to get a concrete functional form of  $Q^2$  dependence for Reggeon form factors in the perturbative region. Hence, the only functional uncertainties in the scattering amplitudes is the on-shell Reggeon form factors and Regge trajectories. However, these functions must be the same as for the corresponding elastic scattering and, so, the concrete applications of the colour dipole approach to the vector meson electroproduction must be supplemented by the simultaneous description of the high-energy proton-(anti)proton diffractive scattering with the same Regge trajectories and form factors of the proton. This has not been done in [24, 25]. Nevertheless, the colour dipole approach is still the only existing method for the quantitative estimation of the  $Q^2$  evolution of the off shell Reggeon form factors. By no means is it in contradiction with the phenomenological approach used in our paper (the colour dipole model

allows us to determine the  $Q^2$  dependence while the Regge-eikonal model allows us to determine  $W$  and  $t$  dependence) and a synthesis of these two approaches seems promising for better understanding of the diffraction mechanism.

After obtaining the explicit  $Q^2$  dependence of the Reggeon form factors in the framework of the colour dipole approach the verification of the proposed minimal Regge-eikonal model will become possible not only by fitting to the HERA data at separate values of  $Q^2$  but also by the simultaneous fit to the whole massive of HERA data on  $d\sigma/dt$  and integrated cross sections. Moreover, the model will be useful for predictions of cross sections of the exclusive vector meson photo- and electroproduction in proton-(anti)proton collisions at RHIC, Tevatron, and CERN LHC energies [31] (the absorptive corrections due to the soft Pomeron exchanges between incoming and between outgoing nucleons may be obtained automatically since we know the soft Pomeron trajectory and the corresponding form factor of the nucleon).

## Conclusion

Now we can summarize the results of our analysis.

The successful simultaneous description of the data on elastic proton-(anti)proton scattering [2] and the data on electroproduction of  $\phi$  meson at low values of  $Q^2$  especially at  $Q^2 = 5 GeV^2$  in the framework of the one-Pomeron model is the evidence that the soft Pomeron absolutely dominates not only in the high-energy nucleon-nucleon scattering but also in the low  $Q^2$  electroproduction of light vector mesons at available energies. The results on the description of the high-quality data on integrated cross sections of  $\rho^0$  electroproduction confirm that for electroproduction of light mesons at low  $Q^2$  (about several  $GeV^2$ ) the contribution of the hard Pomeron to the eikonal (Born term) is several times less than the soft Pomeron's one.

The successful description of the  $J/\psi$  photoproduction in the framework of a two-Pomeron model with the hard Pomeron that has the Kirschner-Lipatov asymptotic behavior [5] in the deeply perturbative domain points to the fact that the hard Pomeron has a perturbative nature (contrary to the soft Pomeron) and dominates over the soft Pomeron at high  $Q^2$  and high  $W$  in accord with expectations of the parton model (the smaller residue slope than the soft Pomeron's one results in the domination of the hard Pomeron also at larger  $t$ ).

Among other things, we explicitly demonstrated that neglecting the contribution of Regge cuts is not justified *a priori* and so in any phenomenological model the validity of the Born approximation must be grounded by explicit estimation of absorptive corrections.

Also it was shown that when considering the processes of exclusive vector meson production there is no need to introduce the "effective dependence" of vacuum Regge trajectories on the virtuality of the incoming photon (this idea is very popular; see, for example, [32, 33, 34]). In fact, such a dependence contradicts general principles since the true Regge trajectories are universal analytical functions of one argument and do not depend on the properties of external particles (such as virtuality). This hypothesis is disguised by the approximation  $\beta_P(t, Q^2)W^{2\alpha_P(t)} + \beta_H(t, Q^2)W^{2\alpha_H(t)} \approx \beta(t, Q^2)W^{2\alpha(t, Q^2)}$  which may be valid only in a limited kinematical domain.

Thus, it was shown that at collision energies higher than  $30 GeV$  available data on exclusive diffractive reactions  $\gamma^* + p \rightarrow V + p$  ( $V = \rho^0, \phi, J/\psi$ ),  $p + p \rightarrow p + p$ ,  $\bar{p} + p \rightarrow \bar{p} + p$  may be described in the framework of a simple phenomenological Regge-eikonal model. This was

achieved by using nonlinear Regge trajectories in which their QCD asymptotic behavior was taken into account explicitly. We would like to point out that linear Regge trajectories not only are in contradiction with QCD but even a satisfactory phenomenological description of the available data on  $t$  dependence of exclusive production of vector mesons has not been attained yet within approaches using linear trajectories (other phenomenological models with  $Q^2$ -independent Regge trajectories and acceptable value of  $\chi^2/\text{DOF}$  [22], [23] also use nonlinear approximations to them).

## References

- [1] R.C. Arnold, Phys.Rev. **153** (1967) 1523
- [2] A.A. Godizov, V.A. Petrov, JHEP **07** (2007) 083
- [3] J. Kwiecinski, Phys.Rev. D **26** (1982) 3293  
R. Kirschner, Z.Phys. C **67** (1995) 459
- [4] H. Cheng, T.T. Wu, Phys.Rev.Lett. **22** (1969) 666  
F.E. Low, Phys.Rev. D **12** (1975) 163  
S. Nussinov, Phys.Rev. D **14** (1976) 246  
P.D.B. Collins, P.J. Kearney, Z.Phys. C **22** (1984) 277
- [5] R. Kirschner, L.N. Lipatov, Z.Phys. C **45** (1990) 477
- [6] P.D.B. Collins, E.J. Squires, **Regge Poles in Particle Physics**. Springer-Verlag 1968  
P.D.B. Collins, **An Introduction to Regge Theory & High Energy Physics**.  
Cambridge University Press 1977
- [7] A. Donnachie, P.V. Landshoff, Phys.Lett. B **437** (1998) 408  
A. Donnachie, P.V. Landshoff, Phys.Lett. B **478** (2000) 146
- [8] J.J. Sakurai, Ann.Phys. (NY) **11** (1960) 1  
J.J. Sakurai, Phys.Rev.Lett. **22** (1969) 981
- [9] ZEUS Collaboration (S. Chekanov et al.), Nucl.Phys. B **695** (2004) 3
- [10] ZEUS Collaboration (S. Chekanov et al.), Nucl.Phys. B **718** (2005) 3
- [11] ZEUS Collaboration (S. Chekanov et al.), PMC Phys. A **1** (2007) 6
- [12] V.A. Petrov, *Proc. of the VIth Blois Workshop on Elastic and Diffractive Scattering (20-24 June 1995, Blois, France)*, p. 139
- [13] V.A. Matveev, R.M. Muradyan, A.N. Tavkhelidze, Lett.Nuovo Cim. **5** (1972) 907  
S.J. Brodsky, G.R. Farrar, Phys.Rev.Lett. **31** (1973) 1153
- [14] M. Gell-Mann, F. Zachariasen, Phys.Rev. **124** (1961) 953
- [15] A.P. Szczepaniak, J.T. Londergan, Phys.Lett. B **643** (2006) 17

- [16] V.A. Petrov, A. Prokudin, Phys.Atom.Nucl. **62** (1999) 1562
- [17] A. Donnachie, P.V. Landshoff, arXiv: 0803.0686
- [18] S.J. Brodsky, W.-K. Tang, C.B. Thorn, Phys.Lett. B **318** (1993) 203
- [19] D.V. Shirkov, I.L. Solovtsov, Phys.Rev.Lett. **79** (1997) 1209
- [20] S. Bethke, J.Phys. G **26** (2000) R27
- [21] S.M. Troshin, N.E. Tyurin, Eur.Phys.J. C **22** (2002) 667
- [22] E. Martynov, E. Predazzi, A. Prokudin, Phys.Rev. D **67** (2003) 074023  
R. Fiore, L.L. Jenkovszky, F. Paccanoni, A. Prokudin, Phys.Rev. D **68** (2003) 014005
- [23] R. Fiore, L.L. Jenkovszky, V.K. Magas, F. Paccanoni, A. Prokudin,  
Phys.Rev. D **75** (2007) 116005
- [24] H. Kowalski, L. Motyka, G. Watt, Phys.Rev. D **74** (2006) 074016
- [25] C. Marquet, R. Peschanski, G. Soyez, Phys.Rev. D **76** (2007) 034011
- [26] ZEUS Collaboration (M. Derrick et al.), Phys.Lett. B 377 (1996) 259
- [27] ZEUS Collaboration (S. Chekanov et al.), Eur.Phys.J. C **24** (2002) 345  
H1 Collaboration (A. Aktas et al.), Eur.Phys.J. C **46** (2006) 585
- [28] L.N. Lipatov, Sov.Phys.JETP **63** (1986) 904
- [29] S.P. Baranov, Phys.Rev. D **76** (2007) 034021
- [30] ZEUS Collaboration (M. Derrick et al.), Z.Phys. C **63** (1994) 391  
ZEUS Collaboration (M. Derrick et al.), Z.Phys. C **69** (1995) 39  
H1 Collaboration (S. Aid et al.), Nucl.Phys. B **463** (1996) 3  
ZEUS Collaboration (M. Derrick et al.), Z.Phys. C **73** (1997) 253  
ZEUS Collaboration (J. Breitweg et al.), Eur.Phys.J. C **2** (1998) 247  
ZEUS Collaboration (J. Breitweg et al.), Eur.Phys.J. C **14** (2000) 213
- [31] W. Schäfer, A. Szczurek, Phys.Rev. D **76** (2007) 094014
- [32] L.P.A. Haakman, A. Kaidalov, J.H. Koch, Phys.Lett. B **365** (1996) 411
- [33] S.V. Goloskokov, P. Kroll, Eur.Phys.J. C **42** (2005) 281  
S.V. Goloskokov, arXiv: 0708.4314
- [34] H.G. Dosch, E. Ferreira, Eur.Phys.J. C **51** (2007) 83

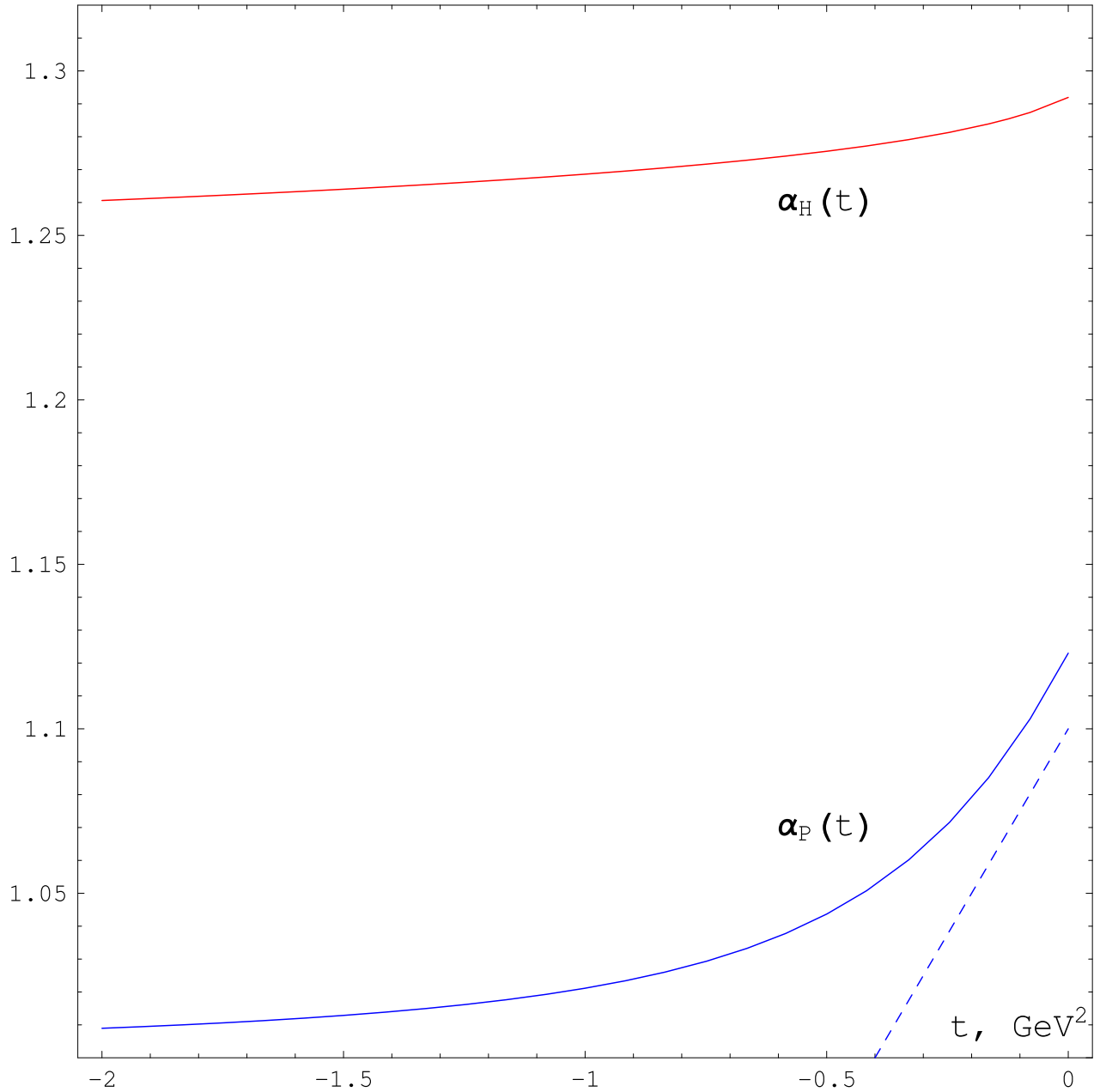


Figure 1: Phenomenological approximations to soft ( $\alpha_P(t)$ ) and hard ( $\alpha_H(t)$ ) Pomeron trajectories obtained correspondingly by fitting the data on high-energy nucleon-nucleon scattering and photoproduction of  $J/\psi$  (dashed line,  $\alpha_P^{lin}(t) = 1.1 + 0.25t$ , is the linear soft Pomeron trajectory usually used in literature).

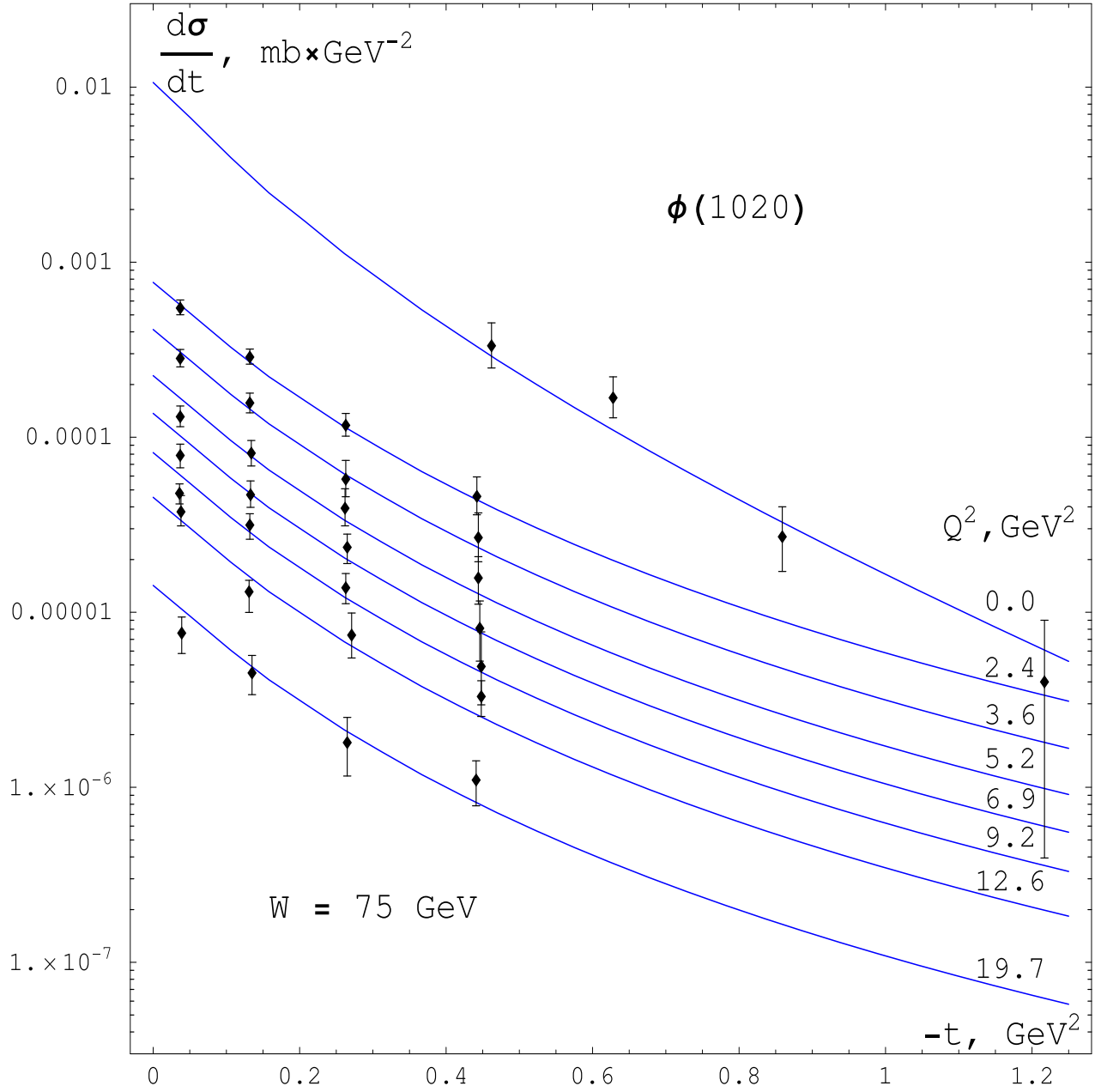


Figure 2: Differential cross sections for exclusive  $\phi$ -meson electroproduction at collision energy  $W = 75 \text{ GeV}$  and different values of the incoming photon virtuality.

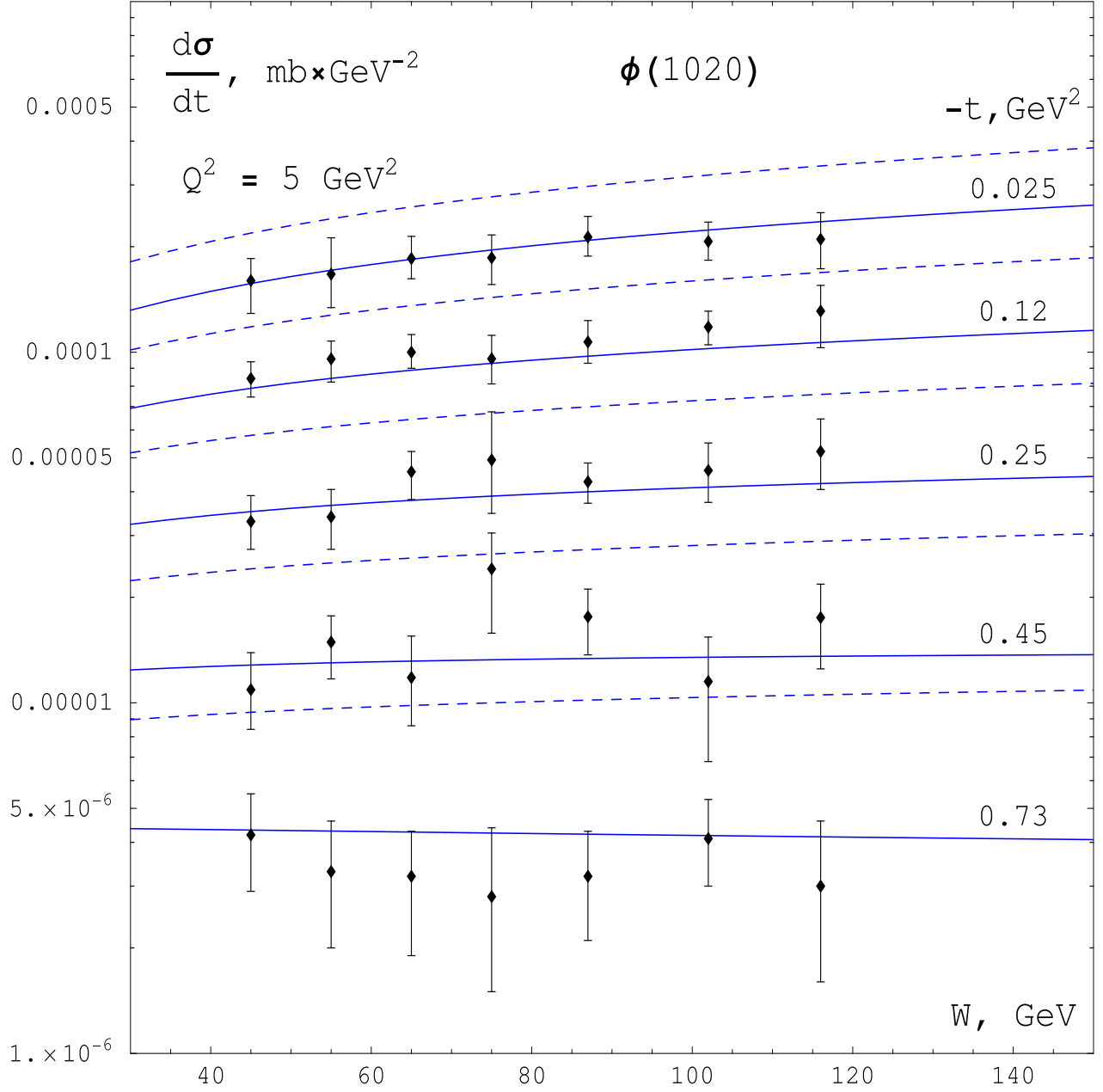


Figure 3: Differential cross sections for exclusive  $\phi$ -meson electroproduction at  $Q^2 = 5 \text{ GeV}^2$  and different values of transferred momentum squared as function of collision energy (1 free parameter, 35 points,  $\chi^2 = 17.5$ ). Dashed lines correspond to cross sections in the Born approximation.



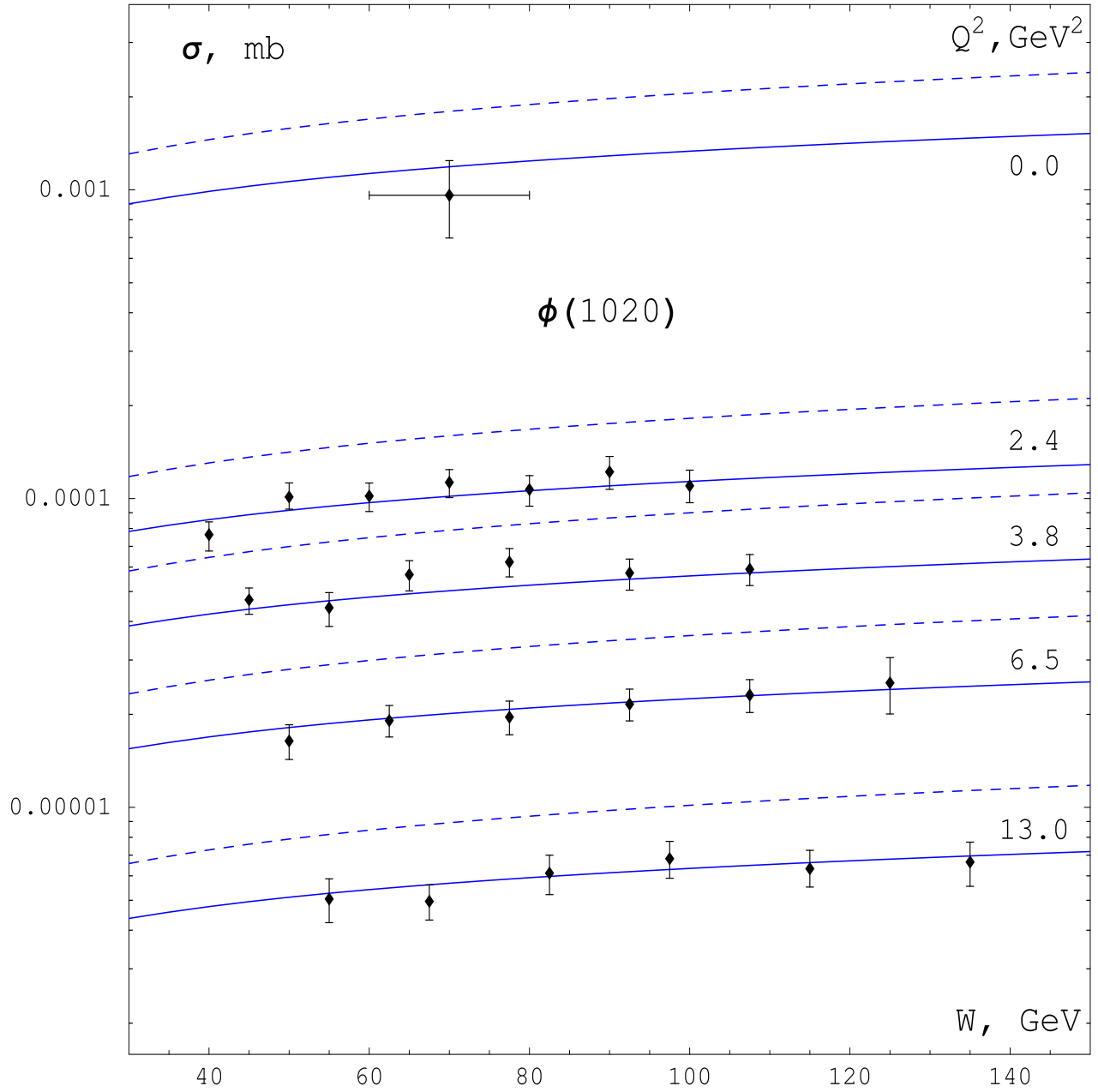


Figure 4: Integrated cross sections for exclusive  $\phi$ -meson electroproduction at different values of the incoming photon virtuality as functions of collision energy. Dashed lines correspond to cross sections in the Born approximation.

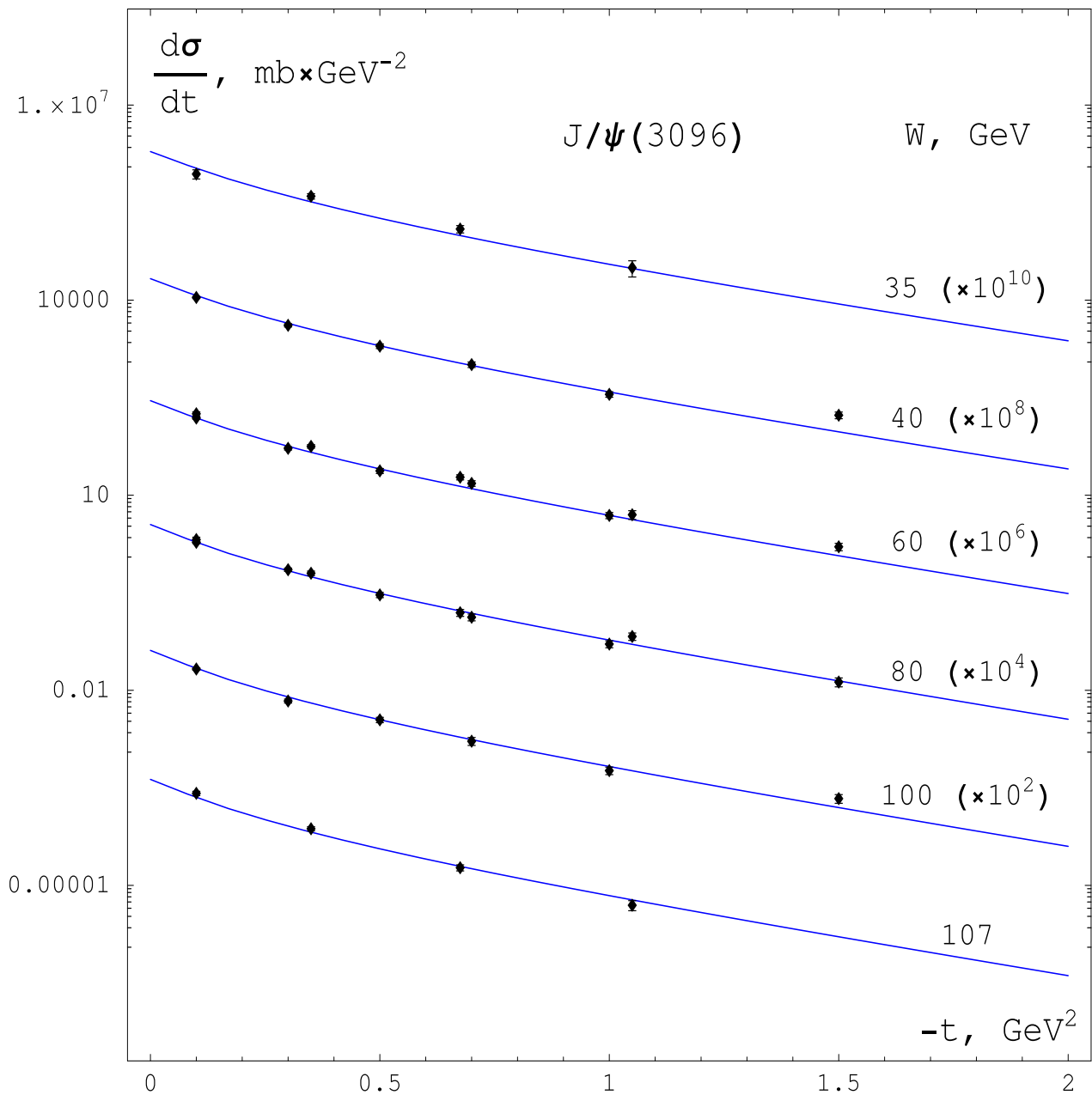


Figure 5: Differential cross sections for exclusive  $J/\psi$ -meson photoproduction at different values of collision energy.

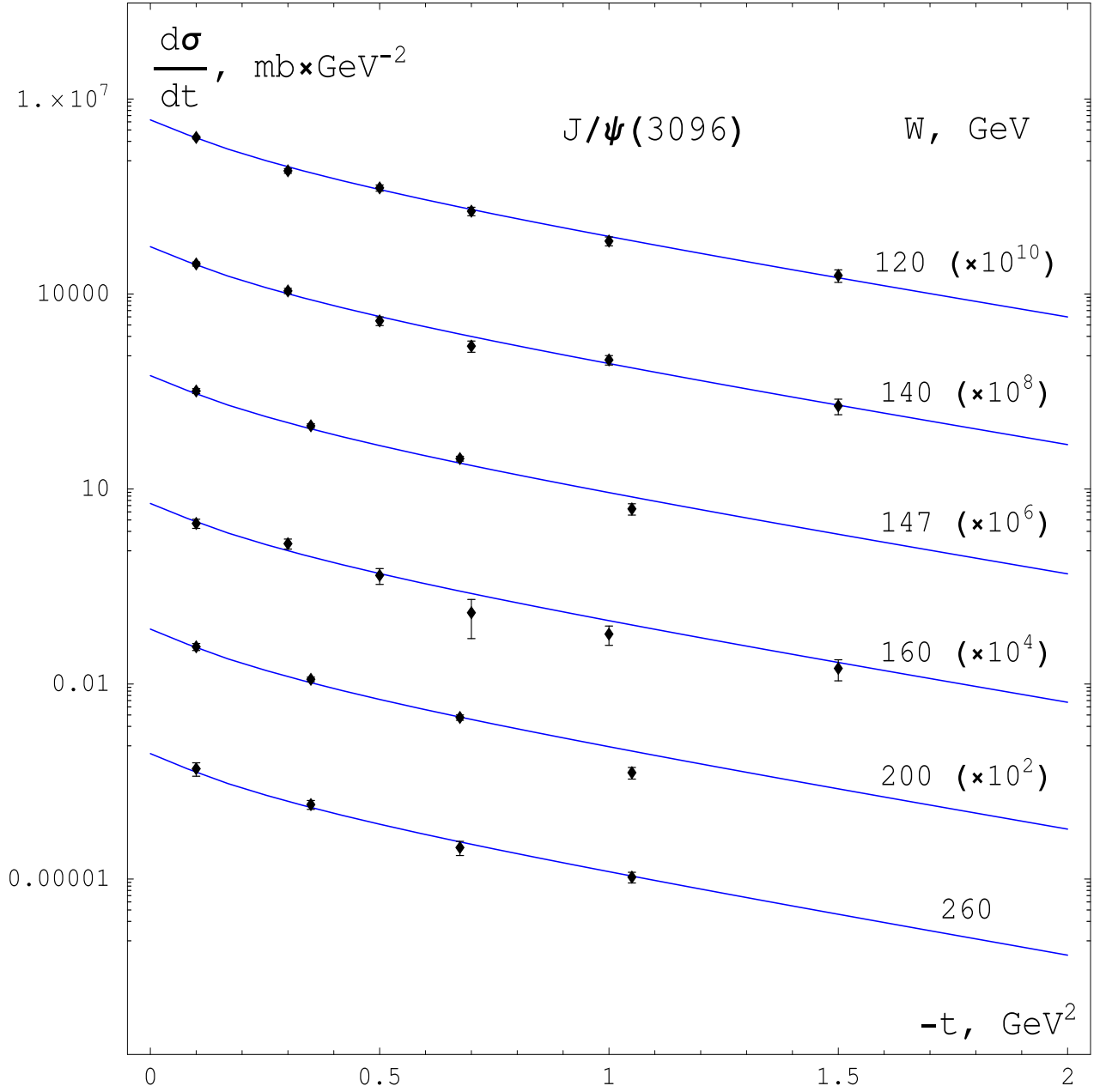


Figure 6: Differential cross sections for exclusive  $J/\psi$ -meson photoproduction at different values of collision energy.

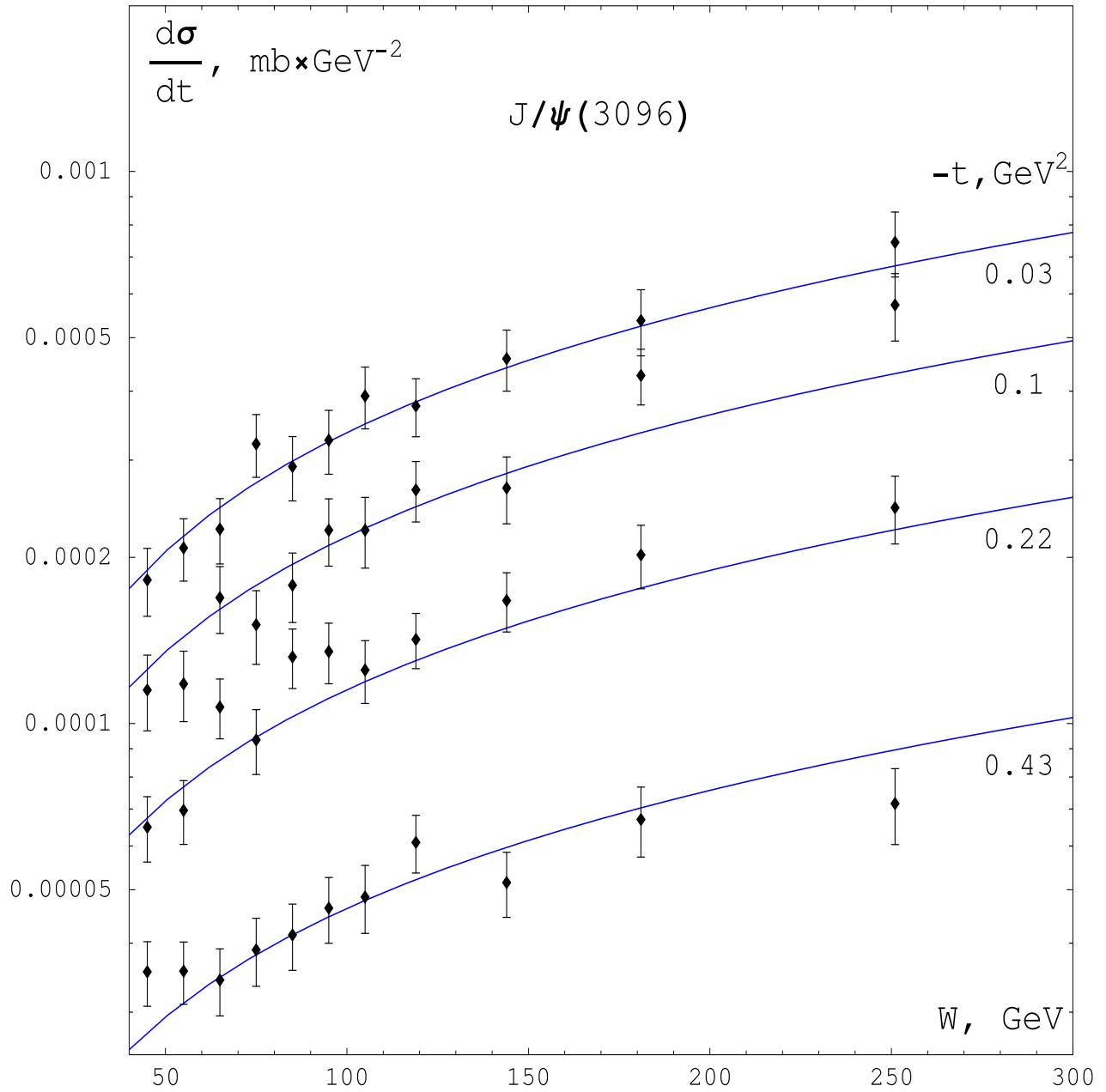


Figure 7: Differential cross sections for exclusive  $J/\psi$ -meson photoproduction at different values of transferred momentum squared as function of collision energy.

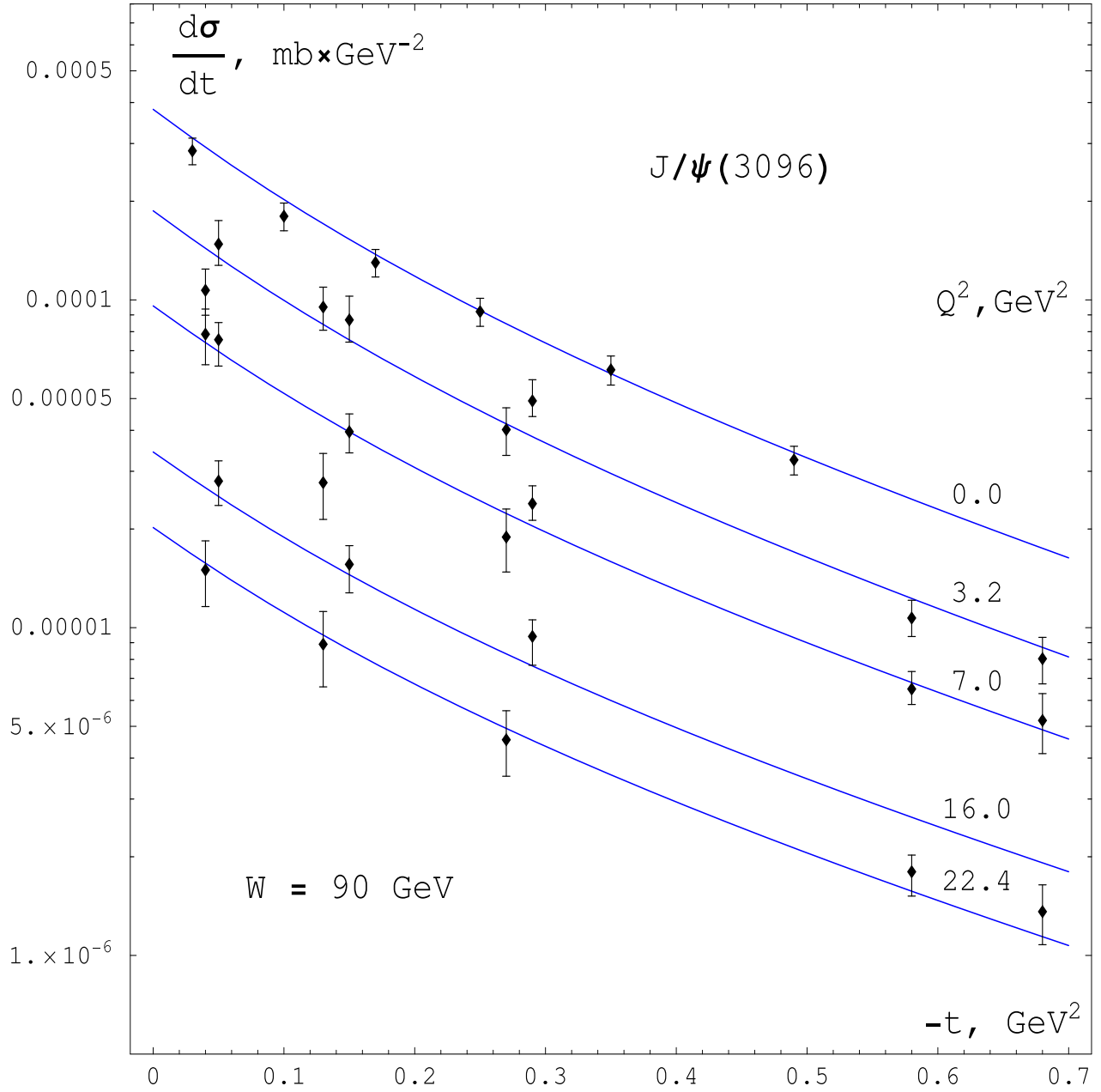


Figure 8: Differential cross sections for exclusive  $J/\psi$ -meson electroproduction at collision energy  $W = 90 \text{ GeV}$  and different values of the incoming photon virtuality.

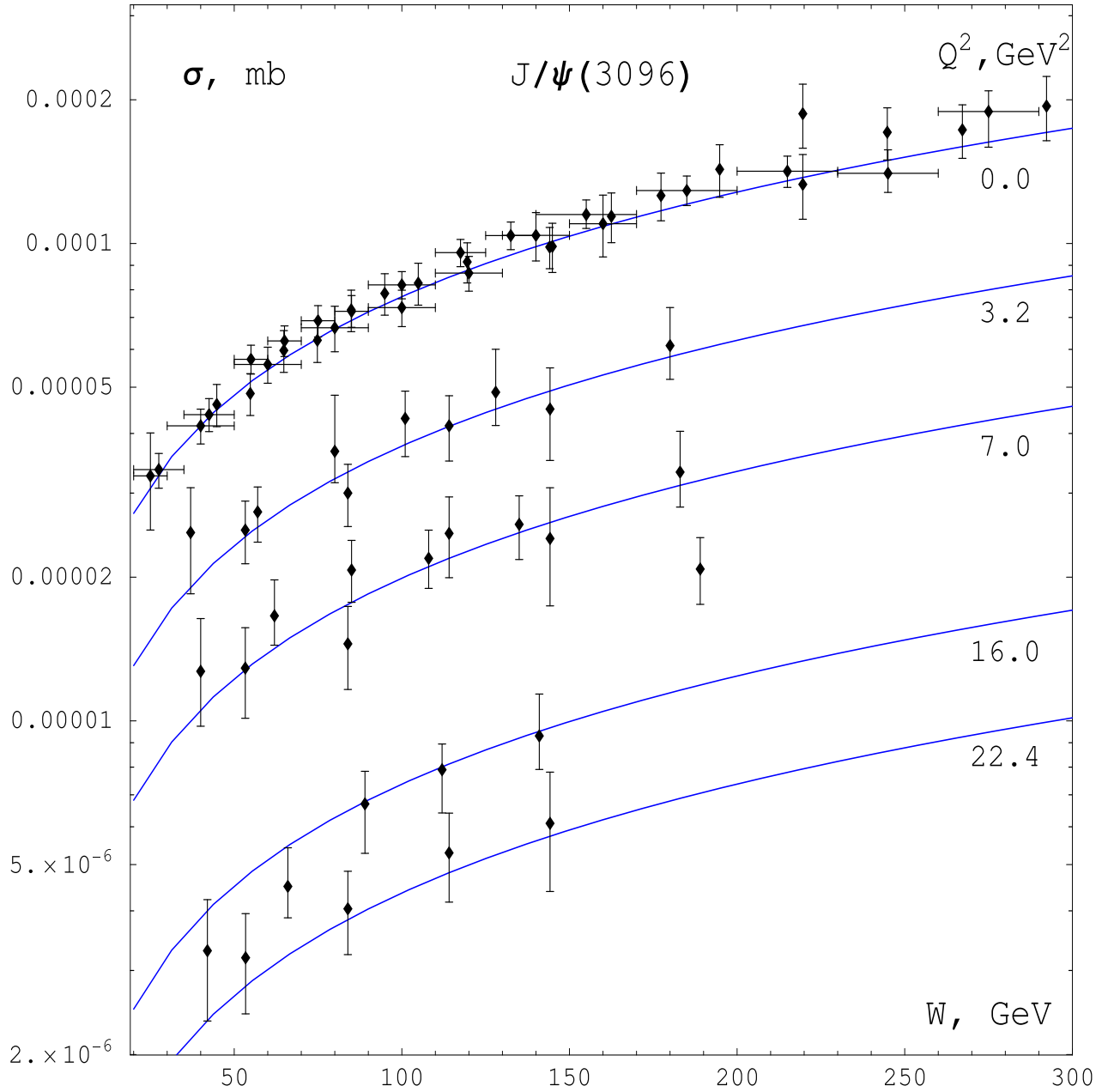


Figure 9: Integrated cross sections for exclusive  $J/\psi$ -meson electroproduction at different values of the incoming photon virtuality as functions of collision energy.

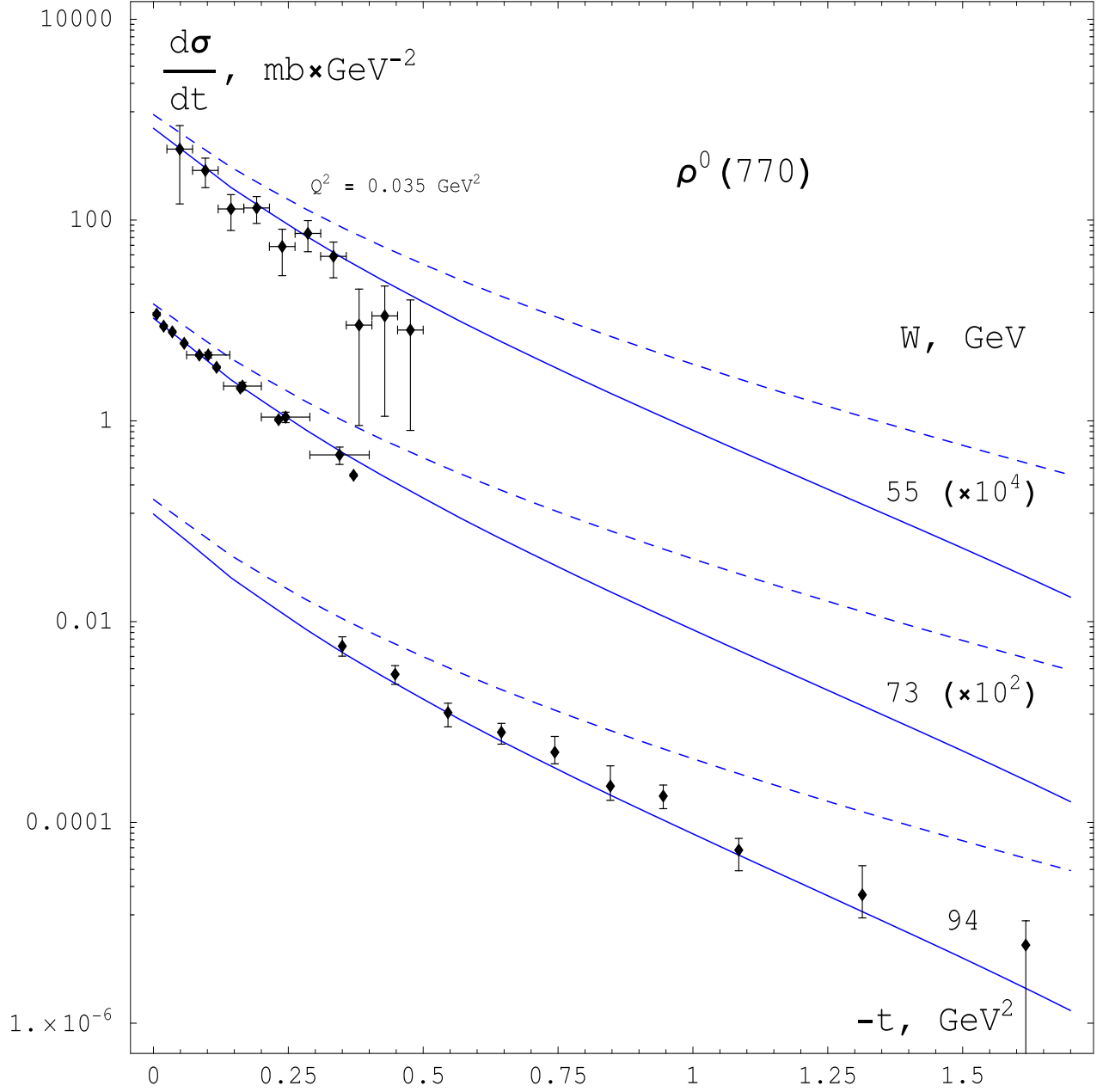


Figure 10: Differential cross sections for exclusive  $\rho^0$ -meson photoproduction at different values of collision energy (the experimental data and the model curve at  $W = 55 \text{ GeV}$  correspond to the incoming photon virtuality  $Q^2 = 0.035 \text{ GeV}^2$ ). Dashed lines correspond to cross sections in the Born approximation.

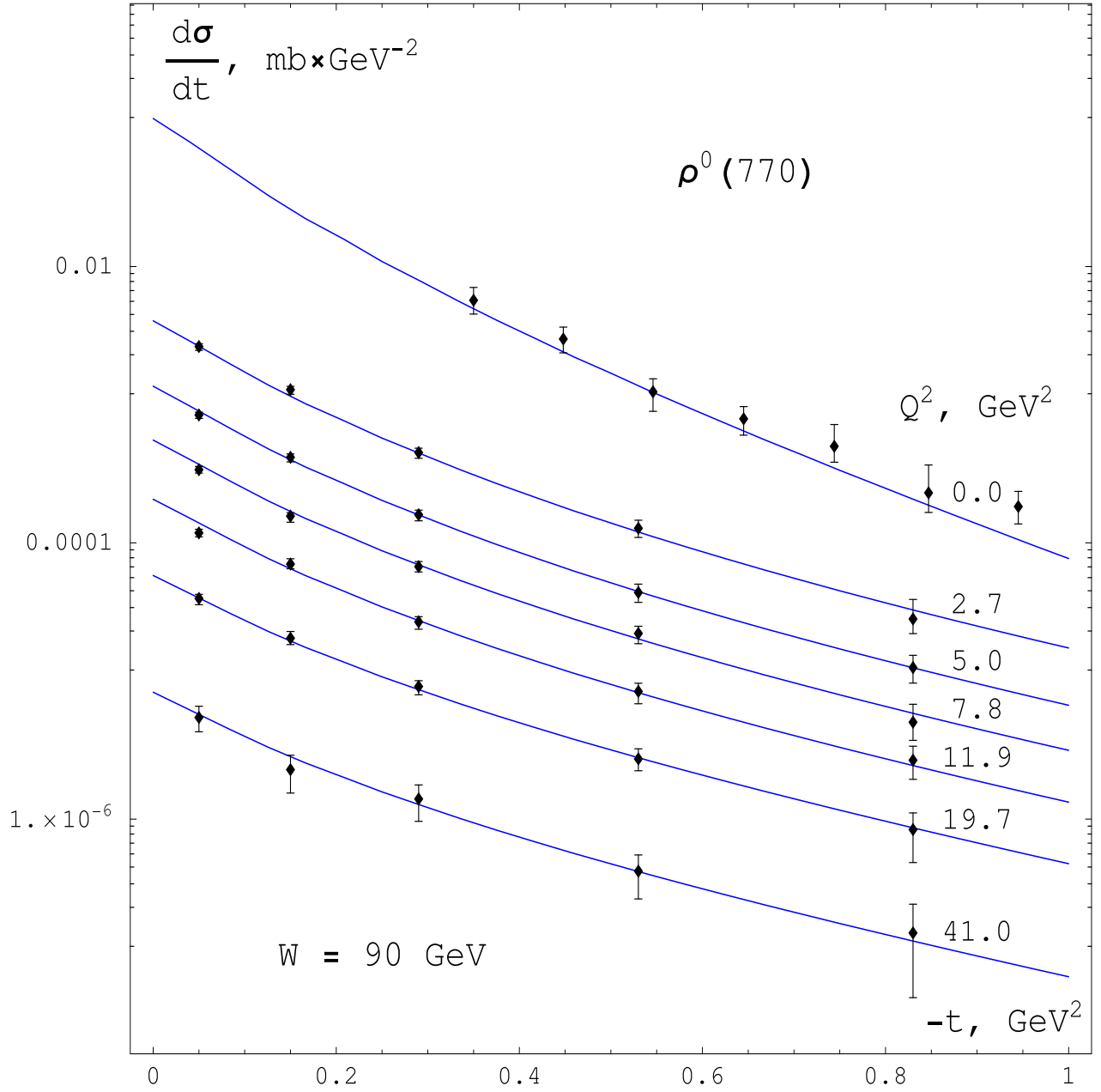


Figure 11: Differential cross sections for exclusive  $\rho^0$ -meson electroproduction at collision energy  $W = 90 \text{ GeV}$  and different values of the incoming photon virtuality.



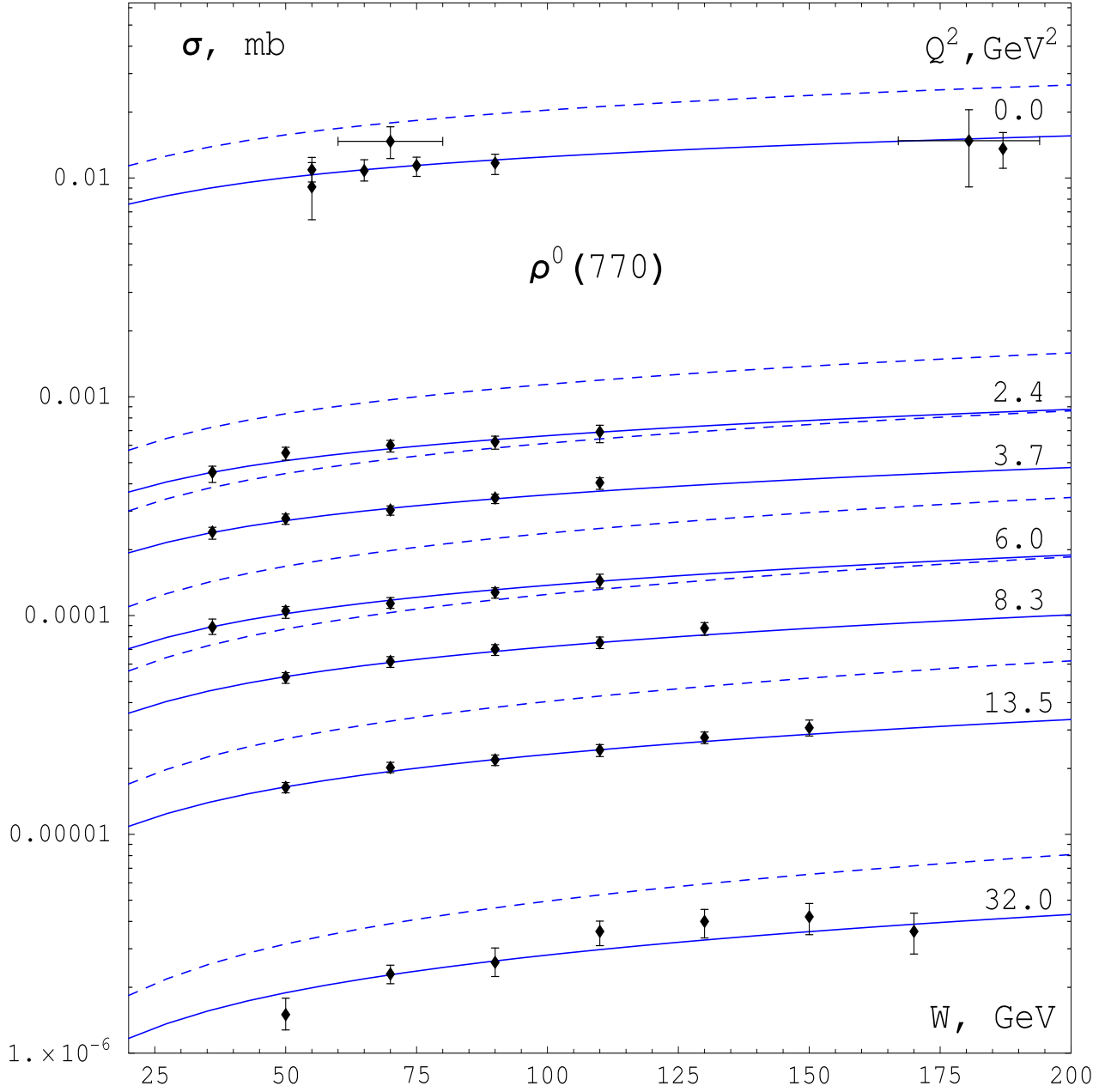


Figure 12: Integrated cross sections for exclusive  $\rho^0$ -meson electroproduction at different values of the incoming photon virtuality as functions of collision energy. Dashed lines correspond to cross sections in the Born approximation.